Int. J. Radiation Oncology Biol. Phys., Vol. 56, No. 1, pp. 259–265, 2003

0360-3016/03/$–see front matter

ELSEVIER

doi:10.1016/S0360-3016(03)00083-X

3D-CRT

PATIENT SETUP ERROR MEASUREMENT USING 3D INTENSITY-BASED IMAGE REGISTRATION TECHNIQUES

SÉBASTIEN CLIPPE, M.D.,*† DAVID SARRUT, PH.D.,† CLAUDE MALET, PH.D.,* SERGE MIGUET, PH.D.,† CHANTAL GINESTET, PH.D.,* AND CHRISTIAN CARRIE, M.D.*

*Department of Radiotherapy, Centre Léon Bérard, Lyon, France; †ERIC Laboratory, Université Lumière Lyon 2, Bron, France

Purpose: Conformal radiotherapy requires accurate patient positioning with reference to the initial three-dimensional (3D) CT image. Patient setup is controlled by comparison with portal images acquired immediately before patient treatment. Several automatic methods have been proposed, generally based on segmentation procedures. However, portal images are of very low contrast, leading to segmentation inaccuracies. In this study, we propose an intensity-based (with no segmentation), fully automatic, 3D method, associating two portal images and a 3D CT scan to estimate patient setup.

Methods and Materials: Images of an anthropomorphic phantom were used. A CT scan of the pelvic area was first acquired, then the phantom was installed in seven positions. The process is a 3D optimization of a similarity measure in the space of rigid transformations. To avoid time-consuming digitally reconstructed radiograph generation at each iteration, we used two-dimensional transformations and two sets of specific and pregenerated digitally reconstructed radiographs. We also propose a technique for computing intensity-based similarity measures between several couples of images. A correlation coefficient, chi-square, mutual information, and correlation ratio were used.

Results: The best results were obtained with the correlation ratio. The median root mean square error was 2.0 mm for the seven positions tested and was, respectively, 3.6, 4.4, and 5.1 for correlation coefficient, chi-square, and mutual information.

Conclusion: Full 3D analysis of setup errors is feasible without any segmentation step. It is fast and accurate and could therefore be used before each treatment session. The method presents three main advantages for clinical implementation—it is fully automatic, applicable to all tumor sites, and requires no additional device.

Patient setup, Image registration, 3D conformal radiotherapy, Correlation ratio, Digitally reconstructed radiographs.

INTRODUCTION

Conformal radiotherapy (RT) is generally chosen because it affords better protection than conventional RT to the normal tissues surrounding the tumor. It also makes it possible to deliver a maximal dose to the tumor and improve the local control rate. Unless high accuracy of the daily patient setup is obtained, this cannot be achieved. The accuracy of the patient setup is thus becoming the limiting factor in 3D conformal radiotherapy (3D-CRT) for which the management of setup errors necessitates margins around the clinical target volume in creating the planned target volume. The optimal position (reference) is defined by the CT scan used for RT planning.

The main difficulty is the day-to-day reproducibility of the patient setup. To check the positioning of patient on the treatment couch, radiation therapists usually use only skin marks. For many years, displacements have been reported. The mean setup error is between 5.5 and 8 mm (1–3), with a maximum, although rarely reported, of 18 mm (4) or 16 mm (5). Even in recent series, using immobilization devices, displacements have remained important: 22% were between 5 and 10 mm (6) and 57% were >4 mm (7). If setup errors have often been measured, their consequences have rarely been evaluated. Three studies have reported a degradation of the therapeutic ratio caused by discrepancies between the planned and delivered treatment positions (8–10).

The first solution proposed to reduce setup errors and their potential serious consequences is patient immobilization. Immobilization devices have proved useful in reducing setup error rates (2, 3, 11, 12). However they do not elim-

Reprint requests to: Sébastien Clippe, M.D., Department of Radiotherapy, Centre Léon Bérard, 28 rue Laennec, 69008 Lyon, France. Tel: 33 47 878 2652; Fax: 33 47 878 2626; E-mail: clippe@lyon.fnclcc.fr

Presented in part at the 3rd S. Takahashi Memorial International Workshop on 3-Dimensional Conformal Radiotherapy, December 8–10, 2001, Nagoya, Japan.

Received Feb 22, 2002, and in revised form Jun 14, 2002. Accepted for publication Jul 3, 2002.

inate all errors, and several recent series failed to find evidence of any improvement with the use of immobilization devices (13, 14).

The second solution to improve patient setup is portal imaging, which is generally used as a complement of immobilization systems. The recently developed electronic portal imaging devices (EPIDs) have several advantages (15–17). First, images are obtained immediately, unlike films that need to be processed. EPIDs thus allow immediate (on-line) setup error detection and correction.

Second, EPIDs provide digital imaging with image processing abilities. Control images are used to detect and quantify setup errors relative to the planned position defined by a reference image. To date, this detection consists only of a visual inspection by the physician. However, visual inspection is inaccurate, time-consuming, and generally done only once a week, at best, in numerous radiation oncology departments to check patient setup. Immediate EPI makes it possible to control patient setup every day before treatment and perform on-line patient setup readjustment before each treatment session. Hence, tools to help physicians in this tedious task are truly needed. Moreover, 3D-CRT uses reduced margins around the target volume. Therefore, accurate patient positioning is essential to ensure that no target is missed and to minimize the risk of local recurrence.

In the present study, a fully 3D and automatic method for the detection of setup errors in conformal radiotherapy is presented. It associates two portal images (PIs) and a CT scan. After setup error estimation, our objective is to correct patient positioning before each treatment session to optimize RT delivery. The final goal of this method is to obtain higher cure rates and higher local control rates with fewer complications.

METHODS AND MATERIALS

Data acquisition and images

The method proposed in this study to determine patient setup errors involves PIs and a RT planning CT scan. Two orthogonal PIs, representing the actual treatment position, and a RT planning CT scan, representing the prescribed treatment position, are compared.

A necessary calibration of the EPID was performed. Our aim was to generate digitally reconstructed radiographs (DRRs) with the same geometric parameters used to acquire PIs. This step was not detailed in this work.

A solid anthropomorphic pelvic phantom was used for simulated treatment (Alderson's phantom, Fig. 1). The first step of the experiment was the acquisition of a CT scan of the phantom using a Picker PQ 2000 CT scanner (Picker International). The CT data were acquired with 3-mm-slice thickness and a 3-mm interval between slices (120 kV and 150 mA). The pixel size of the 512×512 images was 0.87×0.87 mm^2. All experiments were performed using a Sun Ultra Sparc 5 workstation.

The second step of the experiment consisted of positioning the phantom on the treatment couch of the linear accelerator (SL 20, Elekta). The initial position, defined using three laser pointers and skin marks, was the same as in the CT setup. Phantom setup is easier than patient setup because the phantom is motionless, rigid, and flat-bottomed. The phantom was placed in seven positions (six parameters each), using laser pointers and height and width measurements. The precision of the positioning was estimated at about 0.5 mm. Two orthogonal portal images were acquired for each position (0° gantry angle and 90° gantry angle) using an EPID (Iview, Elekta) with a dose rate of 200 monitor units (MU)/min and a total dose of 4 MU/image; 6-MV X-rays were used. The size of the pelvic field was 15×15 cm^2 at the isocenter.

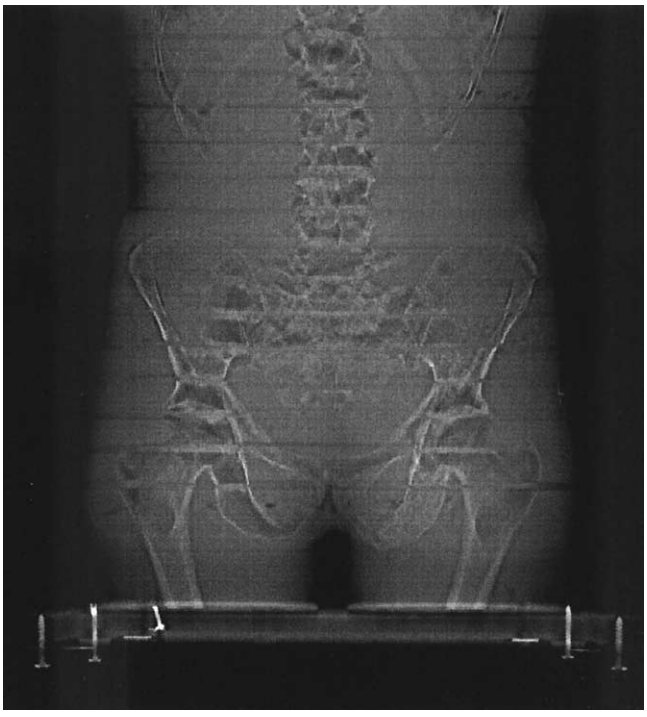

Fig. 1. Radiograph of phantom. Note air between slices.

Goals and methodologic choices

The design of the method had several constraints. It should use equipment available in the hospital: 2 portal imagers and a CT scanner. It should be automatic (i.e., not require human intervention). The registration should be as fast as possible (at least the on-line part), not to keep the patient waiting on the treatment couch. The method should be accurate (millimeter accuracy) to spare normal tissue. Finally, it should be reliable.

We made methodologic choices. First, an "intensity-based" method (without segmentation) was used, rather than a "feature-based" method. Because of their very low contrast, PIs are very difficult to segment. Moreover, the maximization of mutual information of voxel intensities has been demonstrated to be a very powerful criterion for 3D medical image registration (18–20), allowing robust and accurate fully automated registration of multimodal images

(positron emission tomography, CT, and MRI), without the need for image segmentation. Another similarity measure, the correlation ratio, was used by Roche *et al.* (21). A 3D method is necessary because two-dimensional (2D) methods have proved inaccurate and likely to fail, as demonstrated by Hanley *et al.* (22). In the present work, only rigid transformations were considered. Organ motions were not taken into account.

Registration method and estimation of setup errors

The whole method has been previously described in detail (23), in which some theoretical and experimental justifications were given.

Our goal was to register a 3D CT scan, denoted V, according to two 2D projection images (PIs), denoted I_1 and I_2. In this work, we focused on rigid transformations, denoted T, described with six parameters (three translation and three rotation parameters).

The main procedure is an optimization (Eq. 1) over the research space. The objective function, denoted S, measures the "pertinence" of a given position T according to the two projection images. Each iteration consists in measuring the similarity between the two projections observed (I_1 and I_2) and two computed projections (DRRs) of volume V at position T. DRRs are produced using a specific volume-rendering algorithm, from a given projection matrix Q. Q describes both the geometric parameters of the projection and the procedure itself (volume rendering). Each I_i is acquired from a given Q_i, assumed to be accurately determined by a previous calibration procedure. In Eq. 1, the bold letter $\mathbf{I}$ denotes the vector of image I_i, and $\mathbf{Q}T(V)$ the vector of the DRR generated from position T of volume V with the set of projection matrices denoted $\mathbf{Q}$.

$$\hat{T} = \arg \max_{T} S(\mathbf{Q}T(V), \mathbf{I}) \tag{1}$$

The optimization procedure used was the Powell-Brent method (24). The following paragraph presents the quantitative comparisons of two couples of DRRs/PIs, and the next paragraph describes the method used to generate fast, high-quality DRRs.

Similarity measures

DRRs/PIs were compared using intensity-based similarity measures (correlation coefficient, mutual information, or correlation ratio), which do not require any segmentation (25). These measures use all the points in the images and assume there is a statistical link between the intensities of the two images.

Measures can be computed from a 2D co-occurence histogram denoted H: $D_{I_1} \times D_{I_2} \mapsto \mathbb{R}$, where D_{I1} and D_{I2} are the domains of intensity of the two images. The value $H(i, j) = p_{ij}$ is the probability for a coordinate point to have intensity i in the first image and j in the second one. We denoted $p_i = \Sigma_j p_{ij}$ and $p_j = \Sigma_i p_{ij}$ the marginal probabilities. This histogram (sometimes referred to as a joint histogram) is computed by considering each pixel position $\mathbf{x}$ in the overlapping part of the image and updating H according to the intensity value of $i = I_1(\mathbf{x})$and$j = I_2(\mathbf{x})$.

In the global optimization procedure (Eq. 1), the objective function is a single value computed with two couples of images. A unique joint histogram is updated for both couples of images and a single similarity value is computed with this histogram.

The correlation coefficient, chi-square, mutual information, and correlation ratio were used as similarity measures (with the mean $m_I = \Sigma_i i p_i$, the variance $\sigma_I^2 = \Sigma_i (i - m_I)^2 p_i$, the conditional mean $m_{I|j} = \frac{1}{p_j}\Sigma_i i p_{ij}$, and the conditional variance $\sigma_{I|j}^2 = \frac{1}{p_j}\Sigma_i (i - m_{I|j})^2 p_{ij}$):

$$CC(I, J) = \sum_i \sum_j \frac{(i - m_I)(j - m_j)}{\sigma_I \sigma_J} p_{ij} \tag{2}$$

$$\chi^2(I, J) = \sum_i \sum_j \frac{(p_{ij} - p_i p_j)^2}{p_i p_j} \tag{3}$$

$$MI(I, J) = \sum_i \sum_j p_{ij} \log \frac{p_{ij}}{p_i p_j} \tag{4}$$

$$CR(I|J) = 1 - \frac{1}{\sigma_I^2} \sum_j p_j \sigma_{I|j}^2 \tag{5}$$

DRR generation

At each iteration of the main optimization function (Eq. 1) (several hundreds are usually needed), two DRRs must be generated from a position T of the CT volume, according to projection matrix Q. To avoid such time-consuming and expensive generations, the use of precomputed DRRs is proposed. Before the patient comes to receive treatment (off-line, with no important time constraint), two sets of DRRs are generated (one for each projection direction Q_i) by sampling the research space. However, this space, even bounded to the space of plausible projections (e.g., rotations $<10°$ and translations <2 cm) has six dimensions. It is therefore difficult to sample it efficiently. Our solution is to reduce the space from six to two dimensions. Only the two out-of-plane rotations were used to generate this subspace. These are usually the most difficult parameters to retrieve. Then, the use of in-plane (2D) transformations L permits us to obtain the ideal projection Q (T).

Thus, the time-consuming DRR generation is replaced by selecting an image in the set of precomputed DRRs and applying a planar geometric transformation L. To determine which DRR and which transformation L must be used, a geometric least square optimization (Eq. 6) is performed, with a set K of randomly chosen 3D coordinates (composed of 100 points), M is the set of matrices Q' used to precompute DRR.

$$\left.\begin{matrix} L_T \\ Q'_T \end{matrix}\right\} = \arg \min_{L,Q' \in M} \sum_{\mathbf{x} \in K} [QT(\mathbf{x}) - LQ'(\mathbf{x})]^2 \tag{6}$$

Table 1. Root mean square error of estimated position according to each similarity measure for seven positions

Position	CC	Chi-square	MI	CR
1	2.4	2.7	1.4	0.9
2	9.7	12.8	21.0	1.9
3	2.5	15.9	2.8	2.4
4	2.5	1.1	2.6	2.0
5	3.6	7.2	5.3	2.7
6	5.3	3.3	5.8	4.1
7	18.6	4.4	5.1	2.0
Mean	6.0	6.8	6.3	2.3
Median	3.6	4.4	5.1	2.0

Abbreviations: CC = correlation coefficient; MI = mutual information; CR = correlation ratio; RMS = root mean square.
All RMSs are in millimeters.

Optimization was also performed with the Powell-Brent method. In experimental tests, the subspace of out-of-plane rotations is bounded to rotations between $-7°$ and $+7°$ (which is greater than the usually observed displacements [6]) sampled every 0.5°. This method yields 30 samples in each dimension to a total of 900 images. All the parameters of the optimization procedures (starting point, ending condition, tolerance) were the same for all the experiments and for all the similarity measures.

Error estimation

In all the results presented, error ϵ_r between the reference standard position T_{ref} and the estimated position $\hat{T}$ determined using our procedure is expressed by the root mean square (RMS). This error (Eq. 7) is the average distance (expressed in millimeters) between a set of points M transformed by T_{ref} and $\hat{T}$. We used 1000 points in M spread inside a cube of 15 mm^3 centered at a simulated target point (tumor). An RMS error of *x mm* means that each point is *x mm* away from the desired position.

$$RMS(T_{ref}, \hat{T}) = \sqrt{\frac{1}{|M|} \sum_{x \in M} [T_{ref}(\mathbf{x}) - \hat{T}(\mathbf{x})]^2} \qquad (7)$$

RESULTS

Setup error estimations (six parameters and RMS error) are shown on Tables 1 and 2. Table 1 shows the RMS error (in millimeters) of the seven positions for each similarity measure. The correlation ratio leads to the best results. Table 2 shows the seven positions, six parameters, and estimated value of each parameter with the correlation ratio. The whole on-line procedure takes about 2–3 minutes (Sun Ultra Sparc 5 workstation).

DISCUSSION

For several years, registration methods have been used to determine patient setup errors. Two main categories are usually reported: methods using a segmentation step, or feature-based methods, and methods with no segmentation step, or intensity-based methods.

Most of the existing methods are feature-based methods. The segmentation step could be done manually or automatically. In 1991, Bijhold *et al.* (26) presented the first method of setup error measurement using PIs and a reference image that was a film. Image segmentation was done manually with a mouse pointer used to delineate the bony outlines visible in the images. Then, only the extracted features were registered. Several methods used anatomic landmarks only, with three (7, 27) or five points (28) matched. The main difficulty was the accurate definition of the corresponding

Table 2. Values of six parameters of rigid transform for each reference position and corresponding estimation

Position	X	Y	Z	θ	ϕ	ψ	RMS error (mm)
Reference	0	−6	0	0	0	0	
Estimate	−0.3	−6.2	−0.5	−0.5	−0.1	−0.2	0.9
Reference	0	6	0	0	0	0	
Estimate	−1.5	6.3	−1.1	0.4	0.0	−0.1	1.9
Reference	−10	0	0	0	0	0	
Estimate	−7.8	0.0	−0.5	−0.5	−0.6	−0.2	2.4
Reference	0	0	7	0	0	0	
Estimate	−0.6	0.7	6.3	−1.3	−0.5	0.2	2.0
Reference	0	0	0	0	−3	0	
Estimate	1.7	−0.4	−0.3	0.5	−4.6	0.7	2.7
Reference	0	0	0	0	0	5	
Estimate	−2.7	0.5	−0.6	−0.7	0.3	2.2	4.1
Reference	−4.0	−4.0	4.0	0.0	−4.0	4.0	
Estimate	−4.0	−4.6	3.5	0.4	−5.4	3.1	2.0

Abbreviation: RMS = root mean square.
Coordinate system is attached to the gantry: X-axis in lateral direction, Y-axis in vertical direction, and Z-axis in longitudinal direction; rotations about the axes X, Y, Z represented by θ, ϕ, ψ (translations parameters in millimeters and rotation parameters in degrees).

points in the two images to be compared. The main drawback of these methods is that they generally consider only in-plane (2D) information, which is now known to be inaccurate in the case of an out-of-plane rotation or a large translation (22, 26, 29, 30). Moreover, the methods proposed were not fully automatic, so they could not be used for daily setup correction.

Hence, 3D methods began to be developed. The first idea was to use several PIs taken from different points of view (27, 31). However, the registration method was still 2D, so it had all the same drawbacks. Real 3D methods used DRRs computed by specific volume rendering from a CT scan of the patient acquired before treatment that defined the planned position. The major constraint was then time. Operators could choose either on-line or off-line DRR generation. In 1996, Gilhuijs *et al.* (32, 33) developed a 3D method with partial DRRs to speed up the process. In 2000, Remeijer *et al.* (30) evaluated this method. They considered that the method was fast, but it had important limitations because of a high failure rate of the segmentation step in the PIs that needed to be corrected manually.

Marker-based registration methods (34, 35) were also available. They consisted of radiopaque markers implanted in the patient's body. However, the markers had to be implanted in the tumor volume itself, an important impediment. The second difficulty of this method was the uneasy detection of these markers on very low-contrast portal images.

The very difficult task of portal image segmentation justified the development of other methods of research. Intensity-based methods were developed. They involved gray level of all the pixels of the images that must be compared. These methods assume there is a statistical link between the pixel values of the images to be compared and that this link is at maximum when the images are registered. First, Dong and Boyer (36) and Hristov and Fallone (37) used the linear correlation coefficient in a 2D method. They applied it to the registration of PIs to DRRs that had been modified to resemble megavoltage images. Recently, mutual information, was used by Wells *et al.* (18) and Maes *et al.* (19). They applied this measure successfully in a similar context of multimodality image registration among positron emission tomography, MRI, and CT. Another similarity measure, the correlation ratio, was recently proposed by Roche *et al.* (21).

In preliminary works (38), we used a similarity measure (mutual information), but we considered both views separately. On tests with synthetic images, the results were excellent, with an RMS error between 0.68 and 1.52 mm. However, in real conditions (Alderson's phantom), the method sometimes failed. Hence, two modifications were introduced. We chose to perform a simultaneous optimization of the two views and use another similarity measure, the correlation ratio (21). Plattard *et al.* (39) also used a similarity measure (mutual information) for registration in RT but only in two dimensions.

The method presented in this article has many advantages that make it suitable for clinical implementation. Because the method is 3D, the problem of "out-of-plane rotations" previously reported by Hanley *et al.* (22) is solved. The geometric transformation decomposition (Eq. 6) allows the use of high-quality DRRs without increasing the computational time; Gilhuijs *et al.* (33) computed partial DRRs. High-quality DRRs allow the reliable estimation of the similarity measure. Moreover, the sets of DRRs have to be computed only once, before the first treatment session, and then can be used each day for on-line registration. The method is fully automatic. Contrary to many other previous methods, it does not need any manual outline, nor human intervention, which is essential for facilitating daily estimations and corrections.

The method does not necessitate any additional device. It requires only two PIs and the RT planning CT scan. This is very important in view of large clinical implementation, because 3D-CRT is becoming more and more expensive. It should also be emphasized that the method can be used for all cancer sites.

However, the method has several drawbacks that need to be corrected before clinical use. A potential drawback could be the need for DRR temporary storage. However, with compressed DRR of 140 kb, we need $900 \times 2 \times 140 = 252$ mb for each patient, which is easily tractable at present. Moreover, once the treatment is completed, the DRR could be removed. The optimization step is not optimal, and its reliability should certainly be improved (by eliminating local maxima). Faster optimization would also be required. The experimental materials used in our experiments also have some drawbacks. The phantom is made of superimposed slices with air between the slices, which generate artifacts on all images (DRRs, PIs) collected for registration (Fig. 1). Those artifacts seem to be responsible for several failures. Moreover, the anthropomorphic phantom we used was very old (about 30 years). Bone cavities are empty, so the bony structures were less opaque than expected.

Time is also a very important factor for clinical implementation. The registration part of our method was slower (about 2–3 min) than general feature-based methods, but it avoided the segmentation step. A recent estimation of the method developed by Gilhuijs *et al.* is given by Remeijer *et al.* (30): it lasts about 10 min, because of the high rate of automatic segmentation failure requiring manual correction before registering. Thus, our whole process is faster. However, the speed of our prototype could be improved (e.g., in the optimization part), by using a different method such as the one proposed by Maes *et al.* (20). It is realistic to hypothesize that the entire process could be shortened to <30 s.

Another major challenge in 3D-CRT is organ motion. Some have used ultrasonography for prostate cancer (40). The technique is very interesting but not applicable to all sites. Also, it requires a specific device used for treating prostate carcinoma only. Another solution for limiting organ motion is breath holding, whether self or active (active breath control) to immobilize supra- and even

infradiaphragmatic tumors (41, 42). A trial on the use of active breath control apparatus has begun in our institution.

The setup error measurement method proposed by us is, to our knowledge, the first totally automatic method. However, these results were obtained with an artificial phantom, without air or feces. Additional works are ongoing to validate this registration method on patients. The daily on-line patient setup estimation and correction protocol would result in a highly significant improvement in setup accuracy. Hence, this would allow the use of smaller margins around the clinical target volume to define the planning target volume. Finally, our method allows true optimization of 3D-CRT because it makes it possible to control and correct a patient's setup daily, an essential prerequisite for safe intensity-modulated RT delivery.

REFERENCES

1. Rudat V, Flentje M, Oetzel D, *et al.* Influence of the positioning error on 3D conformal dose distributions during fractionated radiotherapy. *Radiother Oncol* 1994;33:56–63.
2. Soffen E, Hanks G, Hwang C, *et al.* Conformal static field therapy for low volume low grade prostate cancer with rigid immobilization. *Int J Radiat Oncol Biol Phys* 1991;20:141–146.
3. Rosenthal S, Roach M, Goldsmith B, *et al.* Immobilization improves the reproductibility of patient positioning during six-field conformal radiation therapy for prostate carcinoma. *Int J Radiat Oncol Biol Phys* 1993;27:921–926.
4. Greer P, Mortensen T, Jose C. Comparison of two methods for anterior-posterior isocenter localization in pelvic radiotherapy using electronic portal imaging. *Int J Radiat Oncol Biol Phys* 1998;41:1193–1199.
5. De Neve W, Van den Heuvel F, De Beukeleer M, *et al.* Routine clinical on-line portal imaging followed by immediate field adjustment using a tele-controlled patient couch. *Radiother Oncol* 1992;24:45–54.
6. Mock U, Dieckmann K, Wolff U, *et al.* Portal imaging based definition of the planning target volume during pelvic irradiation for gynecological malignancies. *Int J Radiat Oncol Biol Phys* 1999;45:227–232.
7. Stroom J, Olofsen-van Acht M, Quint S, *et al.* On-line set-up corrections during radiotherapy of patients with gynecologic tumors. *Int J Radiat Oncol Biol Phys* 2000;46:499–506.
8. Kinzie J, Hanks G, McLean C, *et al.* Patterns of care study: Hodgkin's disease relapse rates and adequacy of portals. *Cancer* 1983;52:2223–2226.
9. White J, Chen T, McCracken J, *et al.* The influence of radiation therapy quality control on survival, response and sites of relapse in oat cell carcinoma of the lung. *Cancer* 1982;50: 1084–1090.
10. Carrie C, Hoffstetter S, Gomez F, *et al.* Impact of targeting deviations on outcome in medulloblastoma: Study of the French Society of Pediatric Oncology (SFOP). *Int J Radiat Oncol Biol Phys* 1999;45:435–439.
11. Marks J, Haus A. The effect of immobilisation on localisation error in the radiotherapy of head and neck cancer. *Clin Radiol* 1976;27:175–177.
12. Marks J, Bedwinek J, Lee F, *et al.* Dose-response analysis for nasopharyngeal carcinoma: An historical perspective. *Cancer* 1982;50:1042–1050.
13. Nutting C, Khoo V, Walker V, *et al.* A randomized study of the use of a customized immobilization system in the treatment of prostate cancer with conformal radiotherapy. *Radiother Oncol* 2000;54:1–9.
14. Song P, Washington M, Vaida F, *et al.* A comparison of four patient immobilization devices in the treatment of prostate cancer patients with three dimensional conformal radiotherapy. *Int J Radiat Oncol Biol Phys* 1996;34:213–219.
15. van Herk M, Meertens H. A matrix ionisation chamber imaging device for on-line patient setup verification during radiotherapy. *Radiother Oncol* 1988;11:369–378.
16. Boyer A, Antonuk L, Fenster A, *et al.* A review of electronic portal imaging devices (EPIDs). *Med Phys* 1992;19:1–16.
17. Munro P. Portal imaging technology: Past, present, and future. *Semin Radiat Oncol* 1995;5:115–133.
18. Wells W, Viola P, Atsumi H, *et al.* Multi-modal volume registration by maximization of mutual information. *Med Image Anal* 1996;1:35–51.
19. Maes F, Collignon A, Vandermeulen D, *et al.* Multimodality image registration by maximization of mutual information. *IEEE Trans Med Imag* 1997;16:187–198.
20. Maes F, Vandermeulen D, Suetens P. Comparative evaluation of multiresolution optimization strategies for multimodality image registration by maximization of mutual information. *Med Image Anal* 1999;3:373–386.
21. Roche A, Malandain G, Pennec X, *et al.* Multimodal image registration by maximization of the correlation ratio. Technical Report 3378, INRIA, August 1998.
22. Hanley J, Mageras G, Sun J, *et al.* The effects of out-of-plane rotations on two dimensional portal image registration in conformal radiotherapy of the prostate. *Int J Radiat Oncol Biol Phys* 1995;33:1331–1343.
23. Sarrut D, Clippe S. Geometrical transformation approximation for 2D/3D intensity-based registration of portal images and CT scan. In: Niessen W, Viergever MA, editors. Medical image computing and computer-assisted intervention. Vol. 2208. Lecture notes in computer science. Utrecht, The Netherlands: Springer Verlag; 2001. p. 532–540.
24. Press W, Flannery B, Teukolsky S, *et al.* Numerical recipes in C: The art of scientific computing, 2nd ed. Cambridge: Cambridge University Press; 1992.
25. Roche A, Malandain G, Pennec X, *et al.* The correlation ratio as a new similarity measure for multimodal image registration. In: Niessen W, Viergeven MA, editors. Medical image computing and computer-assisted intervention. Lecture notes in computer science. Cambridge, MA: Springer-Verlag; 1998. p. 1115–1124.
26. Bijhold J, van Herk M, Vijlbrief R, *et al.* Fast evaluation of patient set-up during radiotherapy by aligning features in portal and simulator images. *Phys Med Biol* 1991;36:1665–1679.
27. Van de Steene J, Van den Heuvel F, Bel A, *et al.* Electronic portal imaging with on-line correction of setup error in thoracic irradiation: Clinical evaluation. *Int J Radiat Oncol Biol Phys* 1998;40:967–976.
28. Hunt M, Schultheiss T, Desobry G, *et al.* An evaluation of setup uncertainties for patients treated to pelvic sites. *Int J Radiat Oncol Biol Phys* 1995;32:227–233.
29. Michalski J, Wong J, Bosch W, *et al.* An evaluation of two methods of anatomical alignment of radiotherapy portal images. *Int J Radiat Oncol Biol Phys* 1993;27:1199–1206.
30. Remeijer P, Geerlof E, Ploeger L, *et al.* 3-D portal image analysis in clinical practice: An evaluation of 2-D and 3-D analysis techniques as applied to 30 prostate cancer patients. *Int J Radiat Oncol Biol Phys* 2000;46:1281–1290.
31. Hanley J, Lumley M, Mageras G, *et al.* Measurement of

patient positioning errors in three-dimensional conformal radiotherapy of the prostate. *Int J Radiat Oncol Biol Phys* 1997;37:435–444.
32. Gilhuijs K, van de Ven P, van Herk M. Automatic three-dimensional inspection of patient setup in radiation therapy using portal images, simulator images, and computed tomography data. *Med Phys* 1996;23:389–399.
33. Gilhuijs K, Drukker K, Touw A, *et al.* Interactive three dimensional inspection of patient setup in radiation therapy using digital portal images and computed tomography data. *Int J Radiat Oncol Biol Phys* 1996;34:873–885.
34. Balter J, Lam K, Sandler H, *et al.* Automated localization of the prostate at the time of treatment using implanted radiopaque markers: Technical feasibility. *Int J Radiat Oncol Biol Phys* 1995;33:1281–1286.
35. Vigneault E, Pouliot J, Laverdiere J, *et al.* Electronic portal imaging device detection of radioopaque markers for the evaluation of prostate position during megavoltage irradiation: A clinical study. *Int J Radiat Oncol Biol Phys* 1997;37:205–212.
36. Dong L, Boyer A. An image correlation procedure for digitally reconstructed radiographs and electronic portal images. *Int J Radiat Oncol Biol Phys* 1995;33:1053–1060.
37. Hristov D, Fallone B. A grey-level image alignment algorithm for registration of portal images and digitally reconstructed radiographs. *Med Phys* 1996;23:75–84.
38. Sarrut D, Clippe S. Patient positioning in radiotherapy by registration of 2D portal to 3D CT images by a contend-based research with similarity measures. In: Lemke HU, Vannier MW, Inamura K, Farman AG, Doi K, editors. Computer assisted radiology and surgery. San Francisco: Elsevier Science; 2000. p. 707–712.
39. Plattard D, Champleboux G, Vassal P, *et al.* EPID for patient positioning in radiotherapy: Calibration and image matching in the EntroPID system. In: Lemke H, editor. Computer assisted radiology and surgery. San Francisco: Elsevier Science; 1999. p. 265–269.
40. Lattanzi J, McNeeley S, Donnelly S, *et al.* Ultrasound-based stereotactic guidance in prostate cancer—quantification of organ motion and set-up errors in external beam radiation therapy. *Comput Aid Surg* 2000;5:289–295.
41. Wong J, Sharpe M, Jaffray D, *et al.* The use of active breathing control (ABC) to reduce margin for breathing motion. *Int J Radiat Oncol Biol Phys* 1999;44:911–919.
42. Barnes E, Murray B, Robinson D, *et al.* Dosimetric evaluation of lung tumor immobilization using breath hold at deep inspiration. *Int J Radiat Oncol Biol Phys* 2001;50:1091–1098.